STEPWISE APPROACH TO INSAR PROCESSING OF MULTITEMPORAL DATASETS

A. Refice[(1)], F. Bovenga[(2)], R. Nutricato[(2)]
[(1)]*ISSIA-CNR, Via Amendola 166/5, 70126 Bari (Italy), e-mail: refice@ba.issia.cnr.it*
[(2)]*Dipartimento Interateneo di Fisica, Politecnico di Bari, Via Amendola 173, 70126 Bari (Italy), e-mail: rnutric@tin.it, fabio.bovenga@ba.infn.it*

ABSTRACT

Multi-temporal DInSAR processing techniques aim at monitoring millimetric displacements through periodic detection of vertical movements of the earth surface, on either point or distributed scatterers. Many such techniques benefit from the availability of a set of SAR acquisitions which is completely connected through suitable interferometric pairs. Moreover, many of the above methods require as a pre-processing step the co-registration of long series of SAR images to sub-pixel accuracy. Automation of this processing step is highly desirable for effective applications to surface displacement monitoring.
In this paper an approach to determine the best procedure to connect multi-temporal InSAR datasets is investigated.
The method consists in adopting an a priori measure of image interferogram quality, and then build a minimum spanning tree (MST) connecting all the image points in the space determined by the spatial and temporal baselines.
As a priori measure, a natural choice is that of coherence. We model spatial decorrelation as mainly due to the wavenumber shift effect, and temporal decorrelation as a combination of a seasonal effect plus a decrease of coherence with time. Various examples of MSTs computed using different parameters for these models are shown. Results on a real multi-temporal DInSAR dataset are reported and evaluations of both processing efficiency as well as final data quality are presented.
Experimental tests and results are provided with reference to an ERS-1/2 dataset over the Italian landslide site of Caramanico Terme, involved in the ESA AO3-313 project.

1 INTRODUCTION

In the last years it has been shown that interferometric processing of multi-temporal stacks of SAR images can improve the capability of microwave sensors to estimate ground displacements [1, 2, 3]. Among the most important applications of this approach is the monitoring of millimetric surface movements related to natural hazards such as earthquakes, landslides, subsidences, etc. The displacement information is extracted from the temporal sampling of the differential interferometric phase of a series of interferograms, obtained from the SAR images forming the stack. Many such approaches benefit from the availability of a completely connected set of interferograms, since, whenever this condition is not achieved, a priori assumptions have to be imposed on the temporal trend of the displacements [2, 4]. The usual criterion for the selection of suitable pairs is that of having a sufficient level of interferometric coherence, which is a quantitative measure of the reliability of the interferometric phase. Since InSAR coherence generally degrades as the temporal and orbital separation of the two SAR acquisition increases, most approaches relying on the estimation of the interferometric phase through "conventional" InSAR processing favour the formation of InSAR pairs made of images with small orbital and/or temporal separation. Other multi-temporal InSAR approaches exploit the peculiar characteristics of point targets, whose radar backscattering is practically insensitive to temporal or spatial separation between SAR images.
In both the types of application, there are also two conflicting aspects of the pre-processing phase that must be taken into account, namely the huge computational load and the high accuracy requirements. A typical multi-temporal SAR dataset is composed of several tens of radar images (for example, in the case of the ERS satellites, data archives of the order of 100 images on a given frame/track location are available); for each selected image pair, several pre-processing steps (co-registration, interferogram generation, flat earth phase removal, etc.) have to be performed. The quality requirements for these pre-processing steps are generally high; for instance, co-registration accuracy for InSAR applications must be of the order of a tenth of a pixel; flat-earth removal has to rely on accurate orbital modelling to avoid long-wavelength errors. This time-consuming work can be optimized by reducing the user intervention, by means of an automated implementation of the aforementioned steps.
If interferometric pairs are chosen unsuitably, strong decorrelation effects may force the user to interact often with the processing chain, especially in the co-registration step, to preserve the results accuracy. Moreover, in applications on rural, heavily-vegetated, or generally un-urbanised areas, temporal decorrelation can often completely preclude co-registration at sub-pixel accuracy for some image pairs.

Proc. of FRINGE 2003 Workshop, Frascati, Italy,
1 – 5 December 2003 (ESA SP-550, June 2004) 83_refic

In the literature, several strategies for multiple SAR image coupling are mentioned, which use various minimization criteria to reduce decorrelation effects between the images forming each InSAR pair. For instance, in the Permanent Scatterers technique [1], the co-registration problem is mentioned as one of the most critical steps; in the absence of better criteria, the (single) master can be chosen as the "mass center" of the cloud of points representing the images in the Euclidean 2-D space defined by the spatial and temporal baselines. Then, all other images are co-registered to this single master. In other multi-temporal InSAR processing techniques, the possibility of a stepwise co-registration and DInSAR processing to minimize decorrelation is mentioned [2, 3]. In [5], a formal definition of the two approaches (single-master vs. step-wise, or "cascaded") is given, although only the temporal baseline is minimised in the stepwise implementation. In all these works, the observation that both spatial and temporal decorrelation increase with increasing baseline values is used in an empirical way.

In this paper, a possible approach to determine the best coupling strategy for multi-temporal InSAR datasets is investigated. We use the coherence as a model for the expected quality of InSAR pairs. We introduce a simple a priori modeling of the physical origin of spatial and temporal decorrelation. Then, we set up a completely connected set of image pairs, selecting "close" pairs as those satisfying a criterion of maximization of the model coherence. In such a pairing structure, every image is included in at least an interferogram, and is therefore linked to at least another image. This structure, which constitutes a tree, allows to easily transfer interferometric parameters across the whole image stack (e.g. co-registration coefficients, or detected displacement), thus enabling applications of various multi-temporal DInSAR phase processing techniques based either on point or distributed targets.

We show results of applications of the methodology to a real dataset, both in terms of automation in the co-registration process, and in the overall interferometric quality of the resulting interferogram stack.

2 PROBLEM FORMULATION

For demonstration purposes, we refer in the following to the pre-processing phase of a given stack of SAR acquisitions, and in particular to the co-registration step, although the problem formulation can be used as a general framework for the formation and processing of InSAR image pairs.

2.1 Best path selection

Let us suppose to have a stack of N SAR images. The aim is to perform the co-registration and then resample the images, so as to dispose of a new stack of images resampled in a unique geometry. For typical sizes of the image stacks, i.e. several tens of images, it is unpractical to consider the entire number of possible combinations. Instead, co-registration could be attempted between suitable image pairs. Parameters for resampling, once successfully computed, can be transferred from image to image so that in the end all data are resampled to the geometry of one single acquisition. This single "master" image can be supposed to be chosen according to some criterion, although in the following it is shown that this choice is not critical.

We can represent the images as N points in the 2-D space defined by the geometrical baselines, $b_g(i)$, and temporal baselines $b_t(i)$, $i = 1, \ldots, N$, and connect any couple of points by arcs. A graph is then defined as the set of the points (*nodes*) and of the arcs: $G = \{G_n, G_a\}$. The baselines are defined in some reference frame, e.g. with respect to the orbital position and date of a reference image. The problem is then to find the *best path* connecting all the images. Translating into the graph theory language, we are looking for a *rooted spanning tree* of the graph, which satisfies some requirements concerning the optimisation of the InSAR processing.

A *tree* (or a connected graph without cycles) is a graph in which any two nodes are connected by a single path. A tree with N nodes has N–1 arcs. A *spanning tree* of a graph is a sub-graph containing all the nodes [6]. A *rooted tree* is a tree in which a *root node* has been defined. In fact, in a *rooted directed out-tree* the unique path in the tree from the root to any other node is a direct path and for each node a unique predecessor node can be identified. Given a graph, many *rooted spanning trees* can be defined.

Therefore, in our case, we have to select a tree between all the possible ones. The criterion for selecting the *best rooted spanning tree* (BRST) has to match the requirements for a successful processing step for each of the selected pairs. In general, the BRST will be the one that ensures the shortest connection between successive points according to some distance measure.

Let us associate to each arc between nodes i and j a distance $d(i, j)$ (or cost) defined as a generic function of the spatial and temporal baselines:

$$d(i,j) = f\left[b_g(i), b_g(j), b_t(i), b_t(j)\right]. \tag{1}$$

The length of the spanning tree is the sum of the costs of its arcs. The BRST, consisting of the nodes and arcs subsets $\{T_n, T_a\}$, can be built up through the following algorithm:

1. Create a set G_a containing all the arcs of the graph;
2. Select a root node (*master image*) and create the set T_n containing only this node;
3. Create a set G_n containing all the nodes of the graph except the root;
4. Find the arc a with the optimum distance which connects a node in T_n with a node n in G_n;
5. Move a from G_a to the new set T_a and n from G_n to T_n;
6. Loop the steps 4 and 5 on the elements of G_n until the cardinality of G_n is zero.

The above procedure coincides in fact with *Prim's algorithm* [7], and ensures that, given the node $n(i)$, the arc $a(i, j)$ exists in T_a, and that it connects $n(i)$ to its "nearest neighbour", then satisfying the requirement of the *optimal connection*. It can be shown that the BRST is also the minimum spanning tree (MST). Prim's algorithm can be run in a time which is $O(m + n \log n)$, where m is the number of arcs and n is the number of nodes. It can be shown [8] that the MST is unique if the distances $d(i, j)$ are unique. This is verified in all practical cases, since the probability of having two images with exactly the same temporal and spatial baseline with respect to a third one is negligible. This means that the MST does not depend on the choice of the root tree, and therefore the choice of the initial "master" image in the list is not critical for the technique.

2.2 Optimisation criteria

In eq. (1), the distance $d(i, j)$ is defined in terms of the spatial and temporal baselines of images i and j. The key step in the algorithm building the image tree is the minimization of this distance.

The function $d(i, j)$ should be set to operate on normalized quantities, to avoid inconsistencies. We exploit the normalization properties of the coherence to derive an a-dimensional definition of the distance to be minimised. In doing this, we use a simple a-priori modelling of both the spatial and temporal baseline decorrelation.

Spatial decorrelation is generally due to the so-called wavenumber shift effect [9]. Correlation due to wavenumber spectral identity is usually modelled as a linear decreasing function of the spatial (perpendicular) baseline, from 1 to 0. The zero correlation value is reached when the baseline reaches a critical value, defined as the value at which the spectra of the two SAR images are completely disjoint. Formally,

$$\gamma_g(i,j) = \gamma_g(i-j) = \left[1 - \frac{\left|b_g(i-j)\right|}{b_g^{\text{crit}}}\right] \cdot H\left(b_g^{\text{crit}}\right), \tag{2}$$

where $H(\bullet)$ is the unitary step function, b_g^{crit} is the critical baseline value, equal to about 1100 m for the ERS satellites, and $b_g(i - j)$ indicates the relative baseline between images i and j, i.e. $b_g(i - j) = b_g(i) - b_g(j)$. In practice, for realistic estimation, effects such as the coherence estimation bias should be taken into account; however, to our purpose of simple a-priori modelling for coherence optimization, this is equivalent to selecting a lower critical baseline value.

Modelling of the temporal decorrelation is much more difficult. In this case, no general model exists for the temporal decay of interferometric correlation, since a wealth of electromagnetic scattering mechanisms and surface phenomena are responsible of the observed coherence of a given InSAR pair. Different models of decorrelation are used for forests [10, 11], crops [12], or urban environments [13].

We make some simple working hypotheses, and consider here only two main empirical observations related to temporal decorrelation: one is the fact that coherence between any two SAR acquisitions is generally seen to decrease as a function of their temporal separation, with a trend which can often be associated with a negative exponential [14]; the other is that, in general, image pairs containing acquisitions performed in the cold season show higher coherence than pairs formed between images acquired in the warmer period of the year. In other words, two winter images may show higher coherence and then result in better co-registration performance than two summer images with the same temporal distance. This seasonal effect is usually associated with vegetation growth, and is typical of rural landscapes in temperate climates such as those found in Southern Europe.

Based on these considerations, the following measure is used here for the temporal coherence:

$$\begin{aligned}\gamma_t(i,j) &= \gamma_s(i) \cdot \gamma_s(j) \cdot \gamma_e(i,j) \\ &= \left\{1 - w_s(i) \cdot \cos^2\left[\frac{b_t(i) - b_{\text{ref}}}{\Delta b_0}\pi\right]\right\} \cdot \left\{1 - w_s(j) \cdot \cos^2\left[\frac{b_t(j) - b_{\text{ref}}}{\Delta b_0}\pi\right]\right\} \cdot \exp\left[-\frac{\left|b_t(i-j)\right|}{\Delta b_e}\right]\end{aligned} \tag{3}$$

where the two seasonal contributions (γ_s) are supposed to be periodical functions (squared cosines) with a 1-year period, b_{ref} is a relative yearly reference for the seasonal effect (say 01 January), and Δb_0 is the period for temporal decorrelation, for which we have used the value of 365.242199 days, while $b_t(i)$ and $b_t(j)$ are baselines calculated with respect to a certain fixed reference in time. The temporal contribution is written as a negative exponential function of the relative baseline $b_t(i - j)$, with a decay constant Δb_e. The seasonal contribution is modulated by weights w_s, which control their impact on the overall coherence estimate.

With these expressions for the two contributions, the distance to be minimised can be written as:

$$d(i,j) = 1 - \gamma(i,j) = 1 - \gamma_g(i,j)\,\gamma_t(i,j) \tag{4}$$

where γ_g is given by (2) and γ_t by (3).
It should be stressed that the formulas shown above are not an attempt to accurately model the spatial and temporal behaviour of InSAR coherence; they rather represent an a priori guess on the performances of the considered InSAR processing step (co-registration, displacement estimation, etc.) as a function of their spatial and temporal separation.

3 RESULTS

3.1 Dataset description and parameter choice

A series of 33 ERS-2 SAR images was used to test the approach described above. The images are acquired over central Italy, and include the city of Sulmona and an area affected by landslide phenomena, around the urban center of Caramanico Terme. The approach described above was used to build several connected trees for this image stack. In Figure 1, four MST plots obtained by applying the algorithm described with different parameters for the definition of the distance function are shown. The first example, shown in the top-left graph, is obtained with a value of spatial critical baseline of 1100 m, and a decay constant for the temporal exponential factor of only 1 day. In this case, since temporal decorrelation is supposed to occur at a very fast rate, no pair shows baselines short enough; therefore, the most effective approach is to co-register all images to a unique master. In this case, such master image has been chosen as the "mass center" of the spatial and temporal baselines. The criterion is used here only in an operational way to choose one image out of *N*, since, from the point of view of the distance definition with these parameters, all MSTs are equivalent (i.e. have infinite length), whatever the choice of the master. In the second example, at the top right, the temporal decay

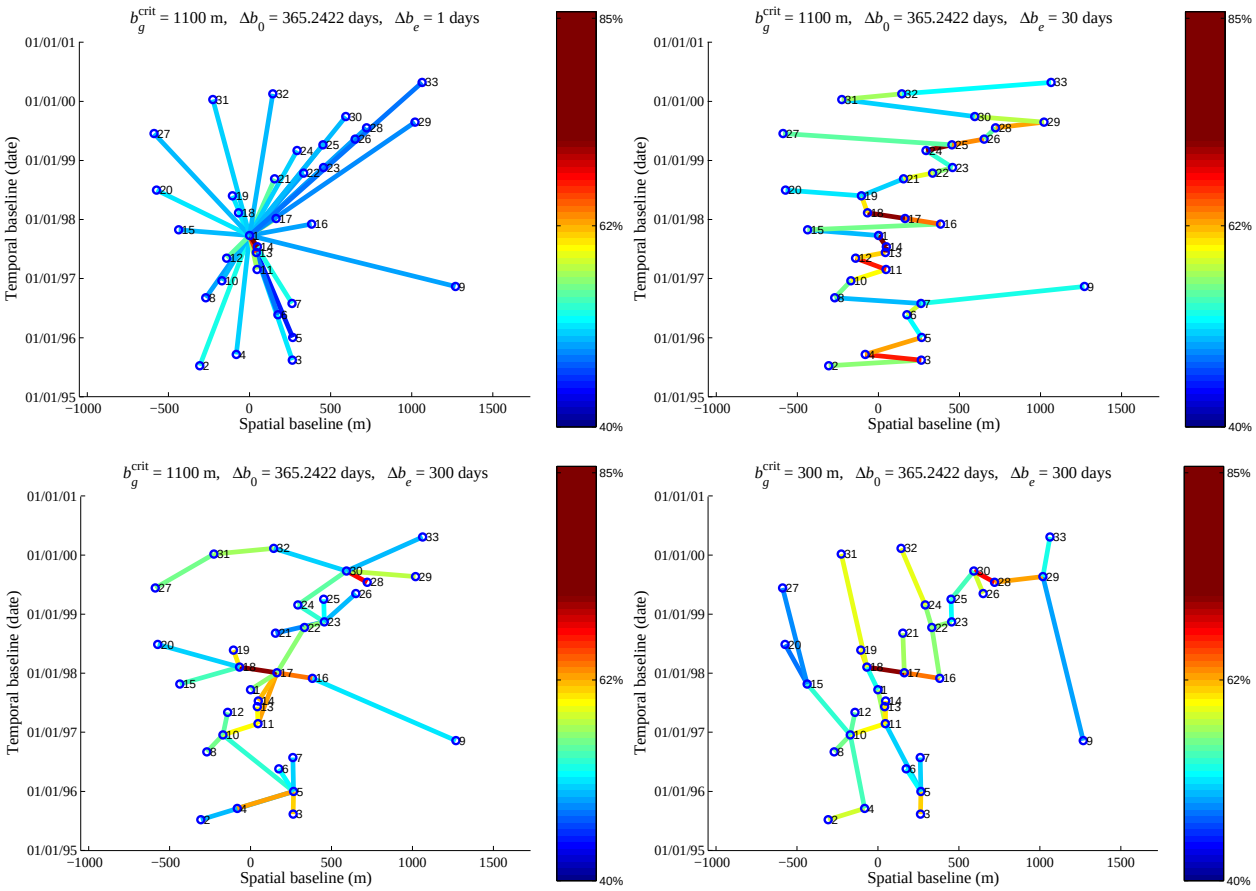

Figure 1. Examples of MSTs obtained with different parameters for the coherence model in eq. (4). The parameter values are shown at the top of each figure. In all cases, $w_s = 0.5$ has been used. The periodic component has in all cases a period of 1 year. The color of each segment encodes a measure of the quality of the co-registration step for that InSAR pair. The adopted merit figure is the fraction of co-registration patches exhibiting a degree of correlation greater than a certain threshold (0.4 in this particular case). Processing is performed with DORIS InSAR software.

constant of the coherence has been changed to 30 days. In this situation, short temporal baselines are privileged with respect to the spatial ones, and therefore the selected MST follows mainly the temporal sequence, with only a few exceptions (i.e. image numbers 9, 20, and 27). The third case (bottom left) has been obtained supposing a temporal decay constant of 300 days. In this case, images are supposed to maintain coherence over longer time spans (which could be the case, e.g. on urban environments); consequently, the effect of the seasonal part of the temporal coherence is relatively stronger, so that "winter" images are privileged and are therefore connected to many other acquisitions. In the last example, the spatial critical baseline has been lowered to 300 m. This forces the MST algorithm to favour short spatial baselines, as can be seen in the bottom-right plot.

3.2 Performance evaluation

The above-mentioned MST approaches have been applied to the actual co-registration of the experimental SAR image dataset. The DORIS software has been used for the image processing [15]. Co-registration of an InSAR pair in DORIS is performed by computing the amplitude correlation between the two images on a certain number of image patches. Wherever the peak correlation values exceeds a certain threshold, the estimated shifts are used to fit a 2-D warp model of the slave image onto the master.

The first evaluation has been made to test the level of automation of the co-registration process, which can be evaluated by computing the relative number of image patches which give a sufficient correlation value in the co-registration process of each pair, and can therefore be used to fit the warp model. This quantity is coded in the color of each arc represented in Figure 1. Work is in progress to test the actual final quality of the co-registration operation, also taking into account the error propagation due to the transfer of the co-registration parameters along the image stack.

It can be seen that the general quality measure for the co-registration process increases progressively passing from the top-left, to the bottom-right plot. In particular, the last plot shows the greatest number of pairs with high percentages of "successful" co-registration patches.

It should be noted that the a priori model of interferogram quality expressed in (4) is related to the phase coherence, whereas the parameter used for the co-registration evaluation in the preceding graphs is the amplitude correlation. However, at least for high values of both quantities, they should agree qualitatively [16, 17].

Another evaluation of the performances of the selected MSTs has been done by using the sample co-registered stacks to locate the permanent scatterer candidates (PSC). This procedure requires as a preliminary step the relative calibration of the image amplitudes [1]. The calibration constants have been computed by using the stepwise approach (i.e. "partial" calibration constants have been computed for the different image pairs and then transferred to the master) with the four MSTs shown in Figure 1. The number of PSC found using the four MSTs, for several amplitude stability thresholds (see [1] for details) are shown in Figure 2. It can be seen that for higher threshold values, the three MSTs with a geometry different from the "single master" show consistent improvement in the PSC detection. The MST corresponding to the bottom-right plot in Figure 1 gives systematically higher numbers of PSC for any threshold values, reaching up to about 12% increase for a threshold of 6.5 (green line with squares). Such an increase can lead to substantial improvements of the performances of the whole PS technique when applied to un-urbanised areas characterised by low densities of stable scatterers [18].

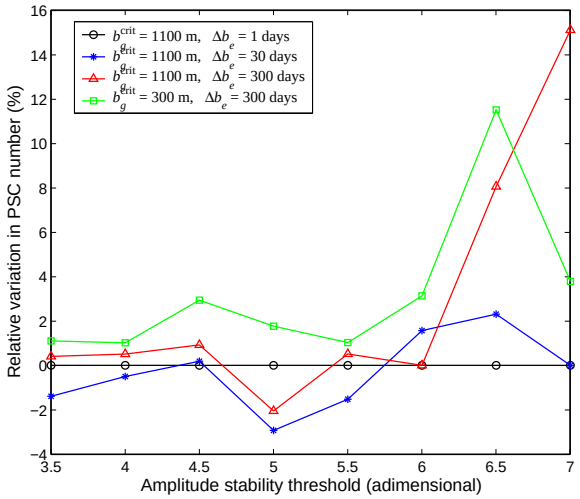

Figure 2. Relative variation of the number of candidate permanent scatterers (PSC) found by processing the experimental data with amplitude relative calibration constants computed through the different MSTs in the stepwise approach. The plots represent the percent variation relative to the "single-master" case, i.e. the top-left MST shown in Figure 1.

4 CONCLUSIONS

A systematic approach to stepwise processing of long series of multi-temporal DInSAR datasets has been presented.The best strategy to couple all the SAR images in pairs is proposed to be that of a minimum spanning tree (MST), which can be shown to optimize "distances" between acquisitions. The actual MST depends on the definition of the distance. For example, models of spatial and temporal expected coherence can be used to derive a priori guess estimates for both geometrical and temporal decorrelation phenomena. Examples are provided of parameter choices favouring short spatial and/or temporal baselines, and including possible seasonal phenomena.

Results on a real multi-temporal DInSAR dataset on a difficult landslide site show some interesting effects of different MST choices on the co-registration and final InSAR quality of the data stacks. In particular, distance measures favouring spatial, temporal or seasonal baselines have been tested. It is found that, on the test dataset, image stacks obtained through MSTs favouring short spatial baselines give better co-registration performances, and also lead to increased numbers of detected candidate stable scatterers when used for amplitude stability thresholding, with respect to a classical "single-master" approach. Awareness of the expected InSAR performance of image pairs, through suitable selection of a guess distance measure to be optimized, could lead to improvements in the operational applicability of multi-temporal InSAR to real sites.
Further work is in progress to better validate the approach and the coherence model adopted, as a function of land cover, scene and environmental conditions.

ACKNOWLEDGEMENTS

ESA is kindly acknowledged for delivery of data, which were provided in the framework of ESA-AO3-313 project, "Application of ERS Data to Landslide Activity Monitoring in Southern Apennines, Italy". Some of the techniques described in the article are also developed in the framework of the EU-funded LEWIS project (www.kinoa.net/lewis).

REFERENCES

[1] A. Ferretti, C. Prati, F. Rocca, "Permanent Scatterers in SAR Interferometry", *IEEE Trans. Geosci. Rem. Sens.*, vol.39, No.1, pp. 8-20, Jan. 2001.

[2] P. Berardino, G. Fornaro, R. Lanari, E. Sansosti, "A new algorithm for surface deformation monitoring based on small baseline differential SAR interferograms", *IEEE Trans. Geosci. Rem. Sens.*, Vol. 40, No. 11, pp. 2375-2383, Nov. 2002

[3] O. Mora, J.J. Mallorqui, A. Broquetas, "Linear and nonlinear terrain deformation maps from a reduced set of interferometric sar images", *IEEE Trans. Geosci. Rem. Sens.*, Vol. 41 No. 10, pp. 2243-2253, Oct. 2003.

[4] M. Costantini, A Amici, F Minati, and L Pietranera, "A Curvature Based Method for Processing of Multi-Temporal SAR Differential Interferometric Measurements", *Proc. of FRINGE'03*, ESA-ESRIN, Frascati (Italy), 1-5 Dec. 2003.

[5] R. Hanssen, D. Moisseev, and S. Businger, "Resolving the acquisition ambiguity for atmospheric monitoring in multi-pass radar interferometry", *Proc. of IGARSS'03*, Toulouse, France, 21-25 July 2003, (CDROM), 4 pages, 2003.

[6] R.K. Ahuja, T.L. Magnanti, J.B. Orlin, *Network Flows –Theory, algorithms and Applications*, Prentice Hall 1993.

[7] R. C. Prim, "Shortest Connection Networks and Some Generalizations", *Bell System Tech. J.* 36, 1389-1401, 1957

[8] E. Horowitz and S. Sahni, *Fundamentals of computer algorithms*, Computer Science Press, 1984.

[9] F.Gatelli A.M.Guarnieri F.Parizzi P.Pasquali C.Prati F.Rocca, "The Wavenumber Shift in SAR Interferometry", *IEEE Trans. Geosci. Rem. Sens.*, Vol.32, No.4, July 1994.

[10] J. O., Hagberg, L. M. H. Ulander, and J. Askne, "Repeat-pass SAR interferometry over forested terrain" *IEEE Trans. Geosci. Rem. Sens.*, Vol. 33, pp. 331– 339, 1995.

[11] J. T. Koskinen, J. T. Pulliainen, J. M. Hyyppä, M. E.Engdahl, and M. T. Hallikainen, "The seasonal behaviour of interferometric coherence in boreal forest", *IEEE Trans. Geosci. Rem. Sens.*, Vol. 39, pp. 820–829, 2001

[12] B. Moeremans, S. Dautrebande, "Soil moisture evaluation by means of multi-temporal ERS SAR PRI images and interferometric coherence", *Journal of Hydrology*, Vol. 234, Issue: 3-4, pp. 162-169, 2000

[13] W.M.F. Grey, A.J. Luckman, D. Holland, "Mapping urban change in the UK using satellite radar interferometry", *Rem. Sens. Env.*, Vol. 87, Issue: 1, pp. 16-22, 2003.

[14] A. Ferretti, C. Colesanti, D. Perissin, C. Prati, F. Rocca, "Evaluating the effect of the observation time on the distribution of SAR Permanent Scatterers", *Proc. of FRINGE'03*, ESA-ESRIN, Frascati (Italy), 1-5 Dec. 2003.

[15] DORIS InSAR processor, on-line: http://www.geo.tudelft.nl/fmr/research/insar/sw/doris/index.html.cgi

[16] A. Monti Guarnieri, C. Prati, "SAR Interferometry: A "Quick and Dirty" Coherence Estimator for Data Browsing", *IEEE Trans. Geosci. Rem. Sens.*, Vol. 35, No. 3, pp. 660-669, May 1997.

[17] R. Touzi, A. Lopes, J. Bruniquel, P.W. Vachon, " Coherence Estimation for SAR Imagery", *IEEE Trans. Geosci. Rem. Sens.*, Vol. 37, No. 1, pp. 135-149, Jan. 1999.

[18] J. Wasowski, A. Refice, F. Bovenga, R. Nutricato, "On the Applicability of SAR Interferometry Techniques to the Detection of Slope Deformations", *Proc. 9th IAEG Congress*, Durban, South Africa, 16-20 September 2002.